trans-Chlorotetracarbonyl(phenylmethylidyne)chromium: Experimental Electron Deformation Density

Anne Spasojević-de Biré,[†] Nguyen Quy Dao,*[,†] Ernst Otto Fischer,[‡] and Niels K. Hansen[§]

Laboratoire de Chimie et Physico-Chimie Moléculaires, ERS 0070 du CNRS, Ecole Centrale Paris, F-92295 Châtenay-Malabry Cedex, France, Anorganisch-Chemisches Institut der Technischen Universität München, Arcistrasse 2, D-8046 München, Federal Republic of Germany, and Laboratoire de Minéralogie, Cristallographie et Physique Infrarouge, URA 809 du CNRS, BP 239, F-54506 Vandœuvre lès Nancy Cedex, France

Received July 23, 1993®

The electron deformation density of the complex $Cl(CO)_4Cr{\equiv}CC_6H_5$ crystallizing in the noncentrosymmetric space group $I4_1md$ was determined at 100 K, using Hansen and Coppens' aspherical atom multipolar model. Positional parameters obtained in this refinement are very close to those obtained by a neutron diffraction experiment recorded at the same temperature. Maps of the electron deformation density show characteristic features of the C≡O and Cr–C ligands interactions, and an important effect of back-bonding between the metal and the carbon atoms is in agreement with the Chatt and Duncanson model. The general features of the different bonds are the same as those which have previously been observed in the methyl homolog but are much better resolved. A conjugation effect between the phenyl ring and the metal–carbyne bond is also experimentally observed. The chromium–carbon triple bond charge appears as a flat and deformed ellipsoid centered near the carbon atom and is very similar to theoretical ab-initio results and thus can be considered as a typical deformation-density feature of the metal–carbyne bond.

Introduction

The first synthesis of transition metal complexes with a formal metal–carbon triple bond was reported by Fischer *et al.*[1] in 1973. Since then, the research on transition metal carbyne (alkylidyne) complexes has rapidly developed because of the great interest in the unusual properties of these compounds, which have been effectively used in various syntheses. It is known that the carbyne radical with its three unpaired electrons is a strong π-acceptor[2] and therefore the M–CO bond in carbonyl (carbyne) complexes (CO being also a π-acceptor) is labilized. It has also been demonstrated that the carbyne complexes are intermediates in catalytic reactions[3] (alkene and alkyne metathesis, alkyne polymerization, ...). For example, in order to understand the reactivity of such compounds, Katz *et al.*[4] have proposed a mechanism for alkyne metathesis with an halogenocarbene unsaturated intermediate, where the initiator is chosen as $Br(CO)_4W{\equiv}CC_6H_5$.

In order to understand the chemical properties of the carbyne complexes, it seems interesting to determine the electron deformation density of some representative carbyne complexes. The crystal and molecular structures of carbyne complexes are regularly studied, and a relatively recent review has been published by Schubert.[5] The M–C(carbyne) bond lengths are ranged between 1.65 and 1.75 Å for the first-row transition metals (Cr, Mn, Fe) and are the shortest observed metal–carbon distances. For a description of structural phenomena in carbyne complexes $L_nM{\equiv}CR$, a conjugation effect between the M≡C and a π-donating substituent can be evoked.[2] The π-bonding between the C(carbyne) atom and one of its substituents (L_nM or R) will change, if the π-donating properties of the other substituents are altered. The general resonant forms can be written as

$$L_nM{\equiv}C{-}R \leftrightarrow L_n\overset{\ominus}{M}{=}C{=}\overset{\oplus}{R}$$

It is difficult to demonstate from structural parameters, especially where the metal–C(carbyne) distance is concerned, if the multiple M≡C bond is conjugated with an organic multiple bond or not, because even if the conjugation effect influences the bond length by changing the order, the multiple bond order of it makes the variation in its length very small and thus unobservable by "classic" X-ray diffraction. However, it has been shown by the molecular orbital calculations that there should be some conjugation effect when multiple bonds are concerned, even with aryl substituents.[6]

For studying such effects experimentally, the electron deformation density obtained by precise X-ray and neutron diffraction on single crystals seems to be one of the best means. In fact, the experimental electron deformation-density maps show not only accurate positions of atoms and consequently the core electron density but also the valence-electron clouds and as such give experimental proof of small charge-transfer phenomena like back-bonding, conjugation, or hyperconjugation effects. The most representative compound of the carbyne series, which is suitable for study by the previously mentioned methods, is *trans*-chlorotetracarbonyl(phenylmethylidyne)chromium (I) of the family $X(CO)_4M{\equiv}CC_6H_5$ (M = Cr, Mo, W; X = Cl, Br, I). I is a particularly good candidate for a charge density study because it crystallizes as big single crystals suitable for a neutron diffraction study.[7] Independently, several conventional X-ray structure determinations have been done for I[8] and for the X = I, M = W[9] and X = Br, M = Cr[8] compounds. The noncentrosymmetric space group of I is also a challenge for crystallographers because it is necessary to determine accurately the phases of the structure factors for the electron deformation density to be informative.

* Author to whom correspondence should be addressed.
† Laboratoire de Chimie et Physico-Chimie Moléculaires.
‡ Anorganisch-Chemisches Institut der Technischen Universität München.
§ Laboratoire de Minéralogie, Cristallographie et Physique Infrarouge.
® Abstract published in *Advance ACS Abstracts,* October 15, 1993.

(1) (a) Fischer, E. O.; Kreiss, G. C.; Kreiter, G.; Müller, J.; Huttner, G.; Lorenz, H. *Angew. Chem.* **1973**, *85*, 618–620. (b) Fischer, E. O. Nobel Speech. *Angew. Chem.* **1974**, *86*, 651–663.
(2) Hoffman, P. *Carbyne complexes*; VCH: New York, 1988; pp 60–98.
(3) Weiss, K. *Carbyne complexes*; VCH: New York, 1988; pp 205–228.
(4) Katz, T. J.; Ho, T. H.; Shih, N. Y.; Ying, Y. C.; Stuart, V. I. *J. Am. Chem. Soc.* **1984**, *106*, 2659–2668.
(5) Schubert, U. *Carbyne complexes*; VCH: New York, 1988; pp 39–58.
(6) Kostic, N.; Fenske, R. *J. Am. Chem. Soc.* **1981**, *103*, 4677–4685.
(7) Nguyen Quy Dao; Neugebauer, D.; Février, H.; Fischer, E. O.; Becker, P. J.; Pannetier, J. *Nouv. J. Chim.* **1982**, *6*, 359–364.
(8) Frank, A.; Fischer, E. O.; Huttner, G. *J. Organomet. Chem.* **1978**, *161*, C27–C30.
(9) Huttner, G.; Lorenz, H.; Gartzke, W. *Angew. Chem.* **1974**, *86*, 667–669.

0020-1669/93/1332-5354$04.00/0

This may be done using aspherical atom models as suggested first by Stewart[10] and then defined by Hirshfeld,[11] Hansen and Coppens,[12] or Craven *et al.*[13] in the LSEXP, MOLLY, and POP programs, respectively.

The aim of this paper is to present the high-resolution X-ray structure of I at low temperature.[14] Using the combination of neutron diffraction results and the Hansen and Coppens'[12] multipole refinement of the X-ray intensities, the experimental electron deformation-density maps are discussed with special emphasis on the nature of the chemical bonds in this complex.

1. Experimental Section

1.1. Data Collection. Single crystals of I for the X-ray diffraction measurements were synthesized in the Anorganisch-Chemisches Institut der TUM (Garching, FRG). The crystal chosen (0.42 × 0.54 × 0.50 mm) was fixed in a Lindeman tube with silicon grease. The low-temperature system (Enraf-Nonius system) providing a cold nitrogen gas stream kept the sample at 110.0(3) K during the measurement. The X-ray diffraction intensities using the Kα radiation of a Mo anticathode (λ = 0.710 69 Å) were recorded with an Enraf-Nonius CAD 4 diffractometer at the SPRSM of the Centre d'Etudes Nucléaires-Saclay, Gif sur Yvette, France). Three reference reflections ((004), (220), (600)) were measured every 1 h to check the stability of the experimental conditions. A very slight decrease of the reference intensity was observed, and correction by interpolation was taken into account for the observed intensities. A total of 3768 reflections (514 reflections observed only once) were recorded by the ψ-scan method (in order to increase the accuracy of the measurements) in the $(\sin\theta)/\lambda$ range between 0.05 and 1.17 Å^{-1}. The crystallographic characteristics of I at 110 K are as follows: space group $I4_1md$, a = 10.045(3) Å, c = 12.002(3) Å, V = 1211.6 Å^3, and Z = 4. The crystal morphology has been determined optically and subsequently refined from 20 ψ-scan measurements. The absorption correction (μ = 12 cm^{-1}) has been done with the FACIES[15] program using a Gauss integration method. The 8 cycles of this refinement (293 observed reflections, 26 parameters, and 6 integration points on each axes) lead to an agreement factor of 5.9%. The data were corrected for Lorentz and polarization effects. The reflections with $I > 2\sigma$ were analyzed using the Lehmann–Larsen algorithm, and for the weaker reflections a fixed background was used. Secondary extinction, using Becker and Coppens'[16] formalism, was found to be negligible. Equivalent symmetry-related reflection intensities were averaged at the end of all correction procedures leading to a lowering of the standard deviations of the data. The final data set consists of 1790 independent reflections with internal agreement factors of $R(F^2)$ = 0.025 and $R_w(F^2)$ = 0.040 for all observations.

1.2. Structural Models and Least-Squares Refinements. In order to determine the electron deformation density, different models have been used for the refinement procedures. In the spherical atom model where the molecules are simply considered as a superposition of atoms with spherical electronic density and anisotropic thermal motions, the atomic scattering form factors were taken as the sum of $f_{core} + f_{valence}$ corresponding respectively to the atomic form factors of the core electrons and of the valence electrons.

In the Hansen and Coppens aspherical atom model[12] with the corresponding computer program MOLLY for the multipolar refinements, the atomic electrons are divided into two parts: one corresponding to the core electrons surrounding the nucleus and the other to the valence electrons. The electronic clouds of the valence electrons have the same forms of the atomic orbitals (the multipolar functions), and their radial extent can be modified. The relative population of these functions and the expansion factor of the various "orbitals" can be determined by refinement.

The electron density ρ_k of each atom k is mathematically expressed[12] by a sum of atom-centered functions:

$$\rho_k(\mathbf{r}) = P_{k,\text{core}}\rho_{k,\text{core}}(\mathbf{r}) + P_{k,\text{valence}}\kappa_k^{3}\rho_{k,\text{valence}}(\kappa_k r) + \sum_{l=0}^{4}\kappa'^{3}_k R_{k,l}(\kappa_k r)\sum_{m=-l}^{+l} P_{k,lm}Y_{k,lm}(\mathbf{r}/r) \quad (1)$$

where ρ_{core} et $\rho_{valence}$ are spherical Hartree–Fock core and valence densities, the Y_{lm} variables are spherical harmonic angular functions in real form, and

$$R_{k,l} = Nr^{n_l}\exp(-\zeta_l\kappa' r)$$

where N is a normalization factor and n_l and ζ_l are chosen for each l value is described previously.[12] $P_{k,core}$, $P_{k,valence}$, $P_{k,lm}$, κ_k, and κ'_k are refinable parameters in addition to the atomic positional and vibrational parameters.

The least-squares refinements of all the reflections for the X-ray data are referred to as **X**, and those of the high-order reflections, only as $\mathbf{X}_{H.O.}$. The multipolar refinements are referred to as **M**. In all the **X**, $\mathbf{X}_{H.O.}$, and **M** refinements, the atomic positions and the thermal parameters of the hydrogen atoms were taken from the neutron diffraction[7] refinement, referred to as **N** in the present paper, as it is clear that the hydrogen atomic parameters cannot be determined accurately by X-ray diffraction due to the small and highly delocalized electron cloud.

The scattering factors were taken from the ref 17a. For the chromium and the chlorine atom we have taken the anomalous scattering factors from ref 17b. The core scattering factors of the chromium atom were assimilated to the 18-electron argon core, those of the chlorine atom to the neon core (10 electrons), and those of the carbon and oxygen atoms to the helium core (2 electrons). For the hydrogen atoms, the contracted atom form factor of Stewart *et al.*[18] was used. Groenewegen *et al.*[19] and Bentley and Stewart[20] have shown that, in the case of bonded atoms, there is both a slight deformation of the core electron cloud (a sharp dipole) and a more diffuse electronic density. The multipole model **M** cannot take into account such a deformation, but the use of the spherical argon core for the chromium ion and the anisotropic thermal parameters can take into account somewhat optimally this situation for the chromium atom. The valence electron form factors were taken as $f_{Cr\ valence} = f_{Cr_{free}} - f_{Cr^{3+}_{Ar\ core}}$ (6 electrons), $f_{Cl\ valence} = {}^1/_7(2\langle j_0\rangle_{3s} + 5\langle j_0\rangle_{2p})$ (7 electrons), $f_{C\ core} = {}^1/_2(\langle j_0\rangle_{2s} + \langle j_0\rangle_{2p})$ (4 electrons), and $f_{O\ core} = {}^1/_3(\langle j_0\rangle_{2s} + 2\langle j_0\rangle_{2p})$ (6 electrons). Initial values of n_l and $\zeta_l\kappa'$ were chosen according to the scheme recommended by Hansen *et al.*[12]: ζ_l constant for all multiple orders of an atom $n_{l(l=1,2)} = 2$, $n_{l(l=3)} = 3$, $n_{l(l=4)}$, and $\zeta_l\kappa' = 3.2$ Å^{-1} for the carbon atom, $n_{l(l=1,2)} = 2$, $n_{l(l=3)} = 3$, $n_{l(l=4)} = 4$, and $\zeta_l\kappa' = 3.4$ Å^{-1} for the oxygen atom, and $n_{l(l=1)} = 2$ and $\zeta_l\kappa = 1.3$ Å^{-1} for the hydrogen atom. We have used the same radial functions $R_{k,l}$ as described by Baert *et al.*[21] for the chromium atom ($n_{l(l=1-4)} = 4$ and $\zeta_l\kappa' = 6.4$ Å^{-1}) and the chlorine atom ($n_{l(l=1-4)} = 4$ and $\zeta_l\kappa' = 5.5$ Å^{-1}).

Concerning the parameters to be determined by least-squares refinements in the **M** procedure, constraints are applied according to the C_{2v} local symmetry of the carbonyl groups and the C_{4v} local symmetry of the chlorine and chromium atoms, in addition to the conditions imposed by the space group symmetry on the density parameters as shown in Figure 1 (the atomic structure being obtained from a previous neutron diffraction

(10) (a) Stewart, R. F. *J. Chem. Phys.* **1969**, *51*, 4569–4577. (b) Stewart, R. F. *J. Chem. Phys.* **1973**, *58*, 1668–1676. (c) Stewart, R. F. *Acta Crystallogr.* **1976**, *A32*, 565–574.

(11) (a) Hirshfeld, F. L. *Acta Crystallogr.* **1971**, *B27*, 769–781. (b) Hirshfeld, F. L. *Isr. J. Chem.* **1971**, *16*, 198–201.

(12) Hansen, N. K.; Coppens, P. *Acta Crystallogr.* **1978**, *A34*, 909–921.

(13) (a) Craven, B. M.; Weber, H. P.; He, X. Tech. Report TR-87-2, Department of Crystallography, University of Pittsburgh, Pittsburgh, PA 15260, 1987. (b) Epstein, J.; Ruble, J. R.; Craven, B. M. *Acta Crystallogr.* **1982**, *B38*, 140–149.

(14) For preliminary results: (a) Nguyen Quy Dao; Spasojević-de Biré, A.; Fischer, E. O.; Becker, P. J. *C. R. Acad. Sci. Paris, Ser. 2* **1988**, *307*, 341–346. (b) Spasojević-de Biré, A. Thesis, University of Paris VI, France, 1989. Spasojević-de Biré, A.; Nguyen Quy Dao; Becker, P. J.; Bénard, M.; Strich, A.; Thieffry, C.; Hansen, N. K.; Lecomte, C. *The Application of Charge Density Research to Chemistry and Drug Design*; Jeffrey, G. A., Piniella, J. F., Eds.; Plenum Press: New York, 1991; pp 385–399. Nguyen Quy Dao *Transition Metal Carbyne Complexes*; Kreissl, F. R., Ed.; Kluwer Academic Publishers: Dordrecht, The Netherlands, 1993; pp 127–129.

(15) Rigoult, A.; Tomas, A.; Guidi-Morisini, C. *Acta Crystallogr.* **1979**, *A35*, 587–590.

(16) (a) Becker, P. J.; Coppens, P. *Acta Crystallogr.* **1974**, *A30*, 129–147. (b) Becker, P. J.; Coppens, P. *Acta Crystallogr.* **1974**, *A30*, 148–153. (c) Becker, P. J.; Coppens, P. *Acta Crystallogr.* **1975**, *A31*, 417–425.

(17) (a) *International Tables for X-ray Crystallography*; Kynoch Press: Birmingham, U.K., 1974; Vol. IV, pp 103–146. (b) *International Tables for X-ray Crystallography*; Kynoch Press: Birmingham, U.K., 1974; Vol. IV, p 149.

(18) Stewart, R. F.; Davidson, E. R.; Simpson, W. T. *J. Chem. Phys.* **1965**, *42*, 3175–3187.

(19) Groenewegen, P.; Zeevalfink, M.; Feil, D. *Acta Crystallogr.* **1971**, *A27*, 487–491.

(20) Bentley, J.; Stewart, R. F. *Acta Crystallogr.* **1974**, *A30*, 60–67.

(21) Baert, F.; Guelzim, J.; Poblet, J. M.; Wiest, R.; Demuynk, J.; Bénard, M. *Inorg. Chem.* **1986**, *25*, 1830–1845.

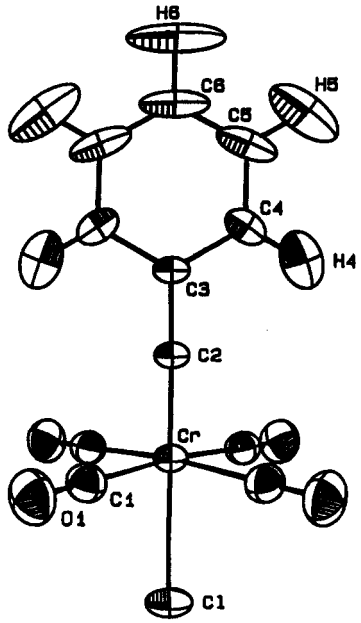

Figure 1. Molecular structure of **1** drawn by ORTEP.[33] The Cl, Cr, C1, C2, C3, C6, and H6 atoms are all arranged along the same *z* axis in special 4*a* position. Surrounding this string of atoms stand C4, H4, C5, and H5 atoms in 8*b* positions. The remaining atoms of the structure are in general positions 16*c*.

study[7]). This will both limit the number of parameters to be refined and reduce the effect of noise in the model deformation-density maps. For the atoms of the asymmetric unit, taking into account their local symmetry, we have defined multiple parameters to the hexadecapolar level for Cr, Cl, C1, O1, C2, and C3, to the octopolar level for C4, C5, and C6, and to the dipolar level for H4, H5, and H6. For the phenyl ring strong deviations from the known density of a nonperturbed ring were observed. During the first eight cycles of refinement, multipole parameters of the carbon atom C4, C5, and C6 were fixed to the values obtained from a multipolar refinement of the phenyl ring of a peptide.[22] These parameters were refined during the next four cycles although the parameters of C2 and C3 had to be fixed to the previous values because of the strong correlation between these values and those of the phenyl ring.

1.3. Electron Deformation Density Maps. In this section, the valence-electron density will be discussed using deformation-density maps. These are defined as the difference between the real electron density in a molecule and the electron density of the promolecule defined as the superposition of spherical free-atom electron densities.[23] The promolecule can be interpreted as the superposition of the electronic clouds of the constituent atoms before the bonding process of the molecule. The difference obtained between these two quantities (real density and promolecule density), which is the deformation density, represents the charge transfer during the molecule-formation process. The positive part represents the gain in electronic density of the bond, and the negative part the loss of the initial valence-electron cloud. The deformation density is meaningful only if the atomic positions of the molecule are very accurately known and if the structure factors (observed) can be properly phased. Three methods can be then used for this: (i) The precise neutron diffraction on a single crystal (N process); (ii) the high-order X-ray refinements ($X_{H.O.}$ refinements), where it can effectively be assumed that, for the high-order reflections, only the core electrons diffract, while the more delocalized valence electrons only contribute to the low-order reflections; (iii) the M refinements.

2. Results and Discussion

Table I summarizes the results obtained for the different refinement procedures (X, $X_{H.O.}$, and M) concerning the agreement factors and the scale factors. The *R* factors are good for all types of refinements but are best for the M models. This is also valid for the goodness of fit indicators. At the same time, the interatomic distances and bond angles (Table II) and also the

Table I. Agreement Factors and Scale Factor of the X-ray Refinements[a]

	X	$X_{H.O.}$	M
$R(F) = \sum_{hkl}(F_o - k\|F_c\|)/\sum_{hkl}F_o$ (%)	3.63	4.82	2.33
$R_w(F) = [\sum_{hkl}w'(F_o - k\|F_c\|)^2/\sum_{hkl}w'F_o^2]^{1/2}$ (%)	3.24	2.12	1.30
$R(F^2) = \sum_{hkl}\|F_o^2 - (k\|F_c\|)^2\|/\sum_{hkl}F_o^2$ (%)	5.86	4.77	2.89
$R_w(F^2) = [\sum_{hkl}w\|F_o^2 - (k\|F_c\|)^2\|^2/\sum_{hkl}w'F_o^4]^{1/2}$ (%)	6.46	4.23	2.60
$GOF = [\sum_{hkl}w(F_o - k\|F_c\|)^2/(NO - NV)]^{1/2}$	6.74	1.58	2.76
NO	1790	1091	1790
NV	50	50	104
NC	4	6	12
k	2.254(3)	2.300(1)	2.252(2)

[a] Definitions and abbreviations: X, spherical atom refinement of all the observations; $X_{H.O.}$, high-order spherical atom refinement $(\sin\theta)/\lambda > 0.8$ Å^{-1}; M, multiple model refinement, where, $w = 1/\sigma^2(F_o^2)$ and $w' = 1/\sigma^2(F_o)$; NO, number of independent reflections; NV, number of variables; NC, number of cycles; *k* scale factor.

Table II. Interatomic Distances (Å) and Bond Angles (deg)[a]

	X	$X_{H.O.}$	N	M
		Interatomic Distances		
Cr–Cl	2.406(1)	2.412(1)	2.410(1)	2.409(1)
Cr–Cl	1.955(1)	1.960(2)	1.955(1)	1.957(1)
C1–O1	1.127(1)	1.128(3)	1.132(3)	1.133(1)
Cr–C2	1.734(2)	1.716(1)	1.725(4)	1.724(1)
C2–C3	1.422(2)	1.431(2)	1.428(6)	1.423(1)
C3–C4	1.408(2)	1.409(2)	1.408(5)	1.409(1)
C4–C5	1.388(2)	1.394(3)	1.383(5)	1.390(1)
C5–C6	1.381(2)	1.398(3)	1.396(4)	1.392(2)
C4–H4	1.090(5)	1.079(5)	1.087(7)	1.086(5)
C5–H5	1.086(6)	1.081(7)	1.081(6)	1.085(6)
C6–H6	1.107(7)	1.099(6)	1.106(8)	1.099(6)
		Bond Angles		
Cl–Cr–Cl	86.95(3)	86.81(2)	86.78(10)	86.90(2)
Cr–Cl–O1	179.73(9)	179.52(18)	179.46(33)	179.72(6)
C2–C3–C4	120.21(9)	119.94(8)	120.16(20)	120.24(5)
C4–C5–C6	120.10(18)	120.23(26)	119.80(27)	120.34(13)
C3–C4–H4	119.57(35)	120.37(35)	119.84(46)	119.92(33)
C4–C5–H5	118.91(37)	119.78(42)	120.11(41)	119.49(35)
C5–C6–H6	119.50(12)	119.87(13)	119.65(22)	119.91(9)

[a] Definitions: X, spherical atom refinement of all the observations; $X_{H.O.}$, high-order spherical atom refinement $(\sin\theta)/\lambda > 0.8$ Å^{-1}; N, neutron diffraction results;[7] M, multipole model refinement.

(22) (a) Souhassou, M.; Lecomte, C.; Blessing, R. H.; Aubry, A.; Rohmer, M. M.; Wiest, R.; Bénard, M.; Marraud, M. *Acta Crystallogr.* **1991**, *B47*, 253–266. (b) Souhassou, M.; Lecomte, C.; Blessing, R.; Aubry, A.; Wiest, R.; Rhomer, M. M.; Bénard, M. *Port. Phys.* **1988**, *19*, 267–273. (c) Souhassou, M. Thesis, University of Nancy I, France, 1988.

(23) When diffraction data are analyzed, the density may be computed by a Fourier synthesis:

$$\Delta\rho(\mathbf{r}) = (1/V)\sum(\mathbf{F}_1/k - \mathbf{F}_2)\exp(-2\pi i\mathbf{H}\cdot\mathbf{r})$$

where *V* is the unit cell volume, *k* is a scale factor, and the meaning of the structure factors $\mathbf{F}_1 = (F_1,\varphi_2)$ and $\mathbf{F}_2 = (F_2,\varphi_2)$ depends on map types.[23] (i) The experimental X–$X_{H.O.}$ deformation density map is calculated with the observed structure factors moduli F_1 and the phase φ_1 of a spherical atom refinement using all the observations; $\mathbf{F}_2$ values are calculated using atomic parameters obtained from a high-order refinement $X_{H.O.}$. (ii) The experimental X–N deformation-density map is calculated with the same $\mathbf{F}_1$ as in the previous map, but the structure factors $\mathbf{F}_2$ are calculated with atomic parameters determined by a neutron diffraction experiment (N). (iii) The experimental X–M deformation density map is calculated with the observed structure factor moduli F_1, with the phase φ_1 from a refined multipole model using all of the observations, and with the structure factors $\mathbf{F}_2$ calculated with spherical atoms defined from atomic parameters of the multipole refinements. The spherical electron cloud is modified by the κ expansion–contraction coefficient refined in the multipole model. (iv) The dynamic multipole deformation density map is obtained with $\mathbf{F}_1$, calculated from the refined multipole model, and the structure factors $\mathbf{F}_2$ of the promolecule as defined for the experimental X–M deformation map. The static density map is calculated directly from the multipole model but without introducing the thermal parameters, thus eliminating the experimental error on these parameters. Residual density maps are calculated with the observed structure factors $\mathbf{F}_1$, the structure factors $\mathbf{F}_2$ calculated from the refined multipole model which also gives the phase φ_1.

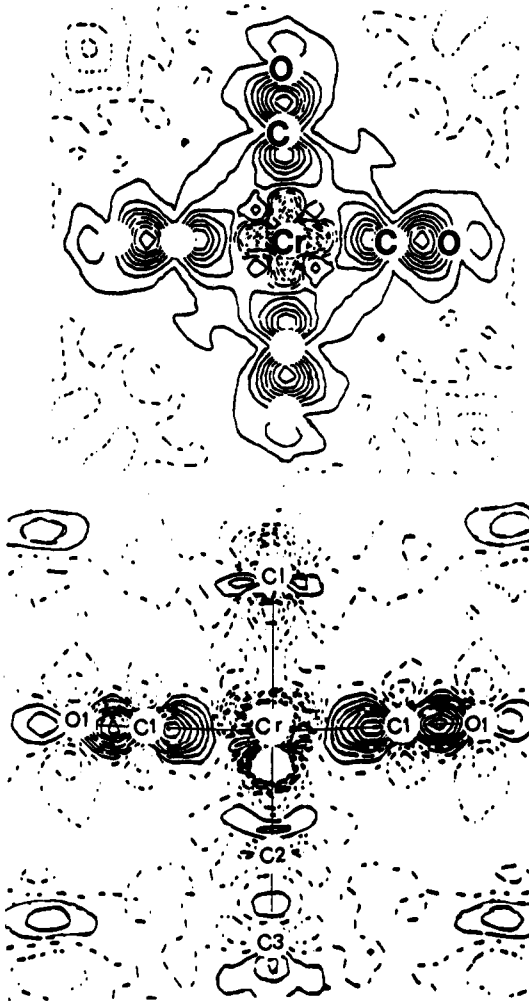

Figure 2. X–M multipole deformation density: (a, top) Plane containing the four carbonyl groups; (b, bottom) plane containing the carbynic bond and two carbonyl groups. The Fourier transform is calculated with $(\sin\theta)/\lambda < 0.9$ Å^{-1} and contours 0.1 e·Å^{-3}.

Table III. Multipole Parameters

	κ	net charge (e$^-$)		κ	net charge (e$^-$)
Cr	1.124(21)	1.08(5)	C4	1.000(4)	−0.36(5)
Cl	1.031(7)	0.16(6)	C5	1.000(4)	0.14(6)
C1	0.977(6)	−0.41(7)	C6	0.976(9)	−0.18(16)
O1	1.005(6)	−0.16(6)	H4	1.000	0.19(3)
C2	1.021(17)	0.08(15)	H5	1.000	0.30(4)
C3	1.038(19)	0.17(16)	H6	1.000	0.45(6)

thermal ellipsoids are, within experimental errors, the same when derived from M and N refinements. This proves that both neutron and X-ray experimental data were of good quality and expecially that they were recorded at the same temperature, which is very important for the X–N study. Tables S1 and S2 (supplementary material) presents the atomic and thermal parameters of different refinements compared to the N refinements. The κ-values and the atomic net charges derived from the M refinements are listed in Table III. The multipole population parameters of different atoms for the M refinements can be found in Table S3. Figure 2 represents respectively the deformation density using the X–M procedure for the two principal sections of the molecule. The residual maps following the multipole refinement (Figure 3) show consistently that the M model has been able to take into account the major part of the information in the diffraction data, except for the density situated on the symmetry elements and near the

(24) Coppens, P. *Electron Distribution and the Chemical Bond*; Coppens, P.; Hall, M. B., Eds.; Plenum Press: New York, 1982; pp 61–100.

Figure 3. Multipole residual density with contours 0.05 e·Å^{-3}; (a, top) Plane containing the four carbonyl groups; (b, bottom) plane containing the carbynic bond and two carbonyl groups.

heavy elements (chromium and chlorine atoms) where the noise level in the residual density is somewhat higher than the estimate based on random errors ($\sigma^2(\rho) \simeq [1/V^2][\Sigma\sigma^2(F)]$), for a general position (σ is modified according to Rees[25]). In a general position $\sigma(\rho) \approx 0.05$ e·Å^{-3}, in a mirror plane 0.07 e·Å^{-3}, and on the symmetry axis 0.10 e·Å^{-3}.

2.1. General Discussion. We shall first make some comments in the atomic structure obtained from various refinements. When compared with the N results,[7] the $X_{H.O.}$ refinement gives relatively better agreement than the X results, while the M models give by far the best agreement.[26] As has been already noted, the interatomic distances calculated from the multipole refinement M are closer to the results obtained from neutron diffraction N than those from the high-order refinement $X_{H.O.}$ (Table II). This shows that the multipole model has eliminated the free atom bias quite efficiently. This is of course to be expected but is clearly demonstrated here.

2.2. Electron Density Distributions. Concerning the electron deformation maps, the X–M and the X–N results are quite similar although there is less noise in the first series of maps (Figure 2b) than in the second series (Figure 4b). This is probably due to

(25) Rees, B. *Isr. J. Chem.* **1977**, *16*, 180–186.

(26) Concerning the $X_{H.O.}$ refinements, different cut-off values (0.65, 0.70, 0.75, and 0.80 Å^{-1}) were tried in the high-order refinement, and finally the highest value was retained as a sufficient number of high-order reflections are still observed and measurable (1091 observed reflections > 3σ for 50 parameters).

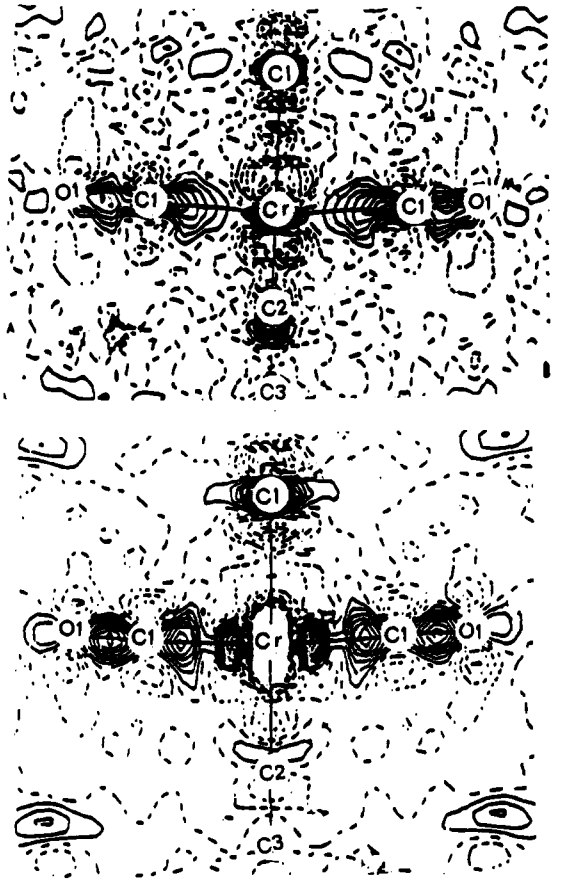

Figure 4. Plane containing the carbynic bond and two carbonyl groups with contours 0.1 e·Å^{-3}: (a, top) X–X deformation density; (b, bottom) X–N deformation density.

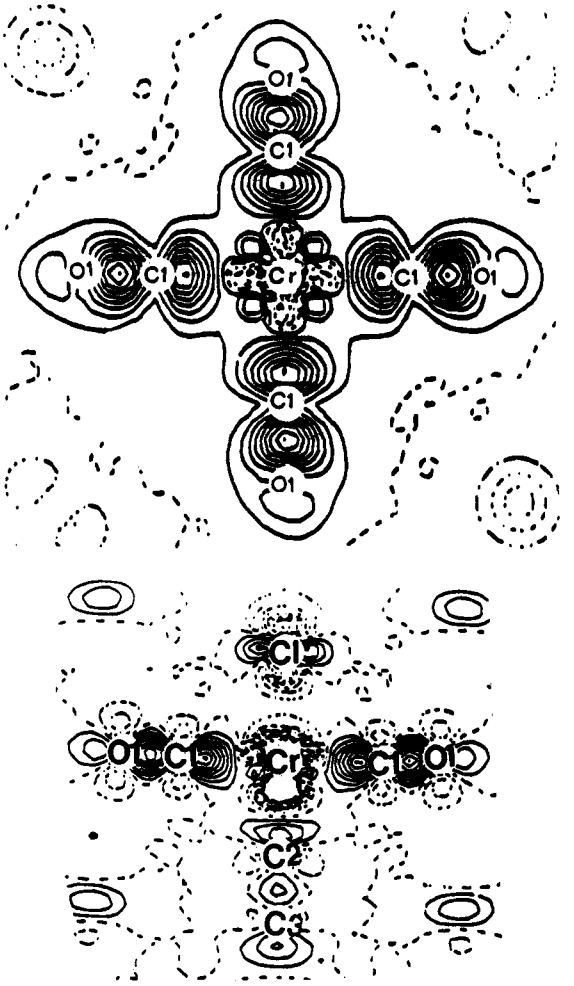

Figure 5. Dynamic multipole model deformation density with contours 0.1 e·Å^{-3}: (a, top) Plane containing the four carbonyl groups; (b, bottom) plane containing the carbynic bond and two carbonyl groups.

the minor difference in the recording temperatures for the X and N results; there may be some indirect cancelation of errors in the X–M maps. As for a comparison of the quality of the different maps, an X–X deformation map is shown in Figure 4a. We shall from now on discuss only the results obtained with the M refinements and the related X–M results. When necessary, the static and the dynamic deformation densities will also be used. As "classic" X-ray and neutron diffraction studies have already shown, I has C_{2v} site symmetry, so the four Cr–C(carbonyl) lengths are equivalent by symmetry as are the four C–O distances. The deviation of the Cl(CO)$_4$Cr group from the ideal C_{4v} symmetry is 0.55°. The dihedral angle of the phenyl plane and the Cl–Cr–C(1) plane is 44.45°. This means that the phenyl group is almost located in a bisecting plane of the CO groups. The CO groups are bent toward the chlorine atom by 3.2(1)°.

Let us first examine the deformation density in the Cr(CO)$_4$ plane for Figure 2a. The multiple C–O bond (triple bond in the case of the gaseous CO) is easily visible in the map. However it is not much stronger than the Cr–C bond. This means in fact that the back-donation bonding between the d_π and p_π orbitals exists and is important. One can also observe this back-bonding at the level of the chromium atom where the d_π lobe is clearly apparent. On the back side of the oxygen atom, the lone pair is also seen. However, it is not very pronounced in the X–M maps. All these effects are much better defined in the dynamic and the static maps shown in Figure 5a and 6a. These features are all in qualitative agreement with previous studies of coordination compounds.[27] In this plane and close to the chromium atom, we observe four peaks in the diagonal *xy* directions (i.e. in the crystallographic mirror planes). The symmetry is nearly ideally 4-fold as already mentioned. This is in agreement with the Chatt and Duncanson[28] model indicating a back-donation effect between the carbonyl group and the metal. We find here results similar to those obtained for complexes containing carbonyl ligands, crystallizing in centrosymmetric space groups,[27,29,30] where the phase problem plays a minor role. The peak centered on the Cr–C line, but closer to the carbon atom, is broader in this plane (Figures 2a, 5a, and 6a) than in the perpendicular plane (Figures 2b, 5b, and 6b) in accordance with the idea of a d_{xy}–ligand π-bond. There is no indication of similar chromium d_{xz} and d_{yz} carbonyl interactions, probably due to the competing strongly covalent Cr≡C bond.

The other important features of bonding are located along the axis of the molecule. Let us examine different maps in a section passing through the axis of the molecule and containing two CO groups (Figures 2b, 5b, and 6b). The density distribution surrounding the chlorine and chromium ions is very clear in the X–M map. The deformation density around the chlorine, perpendicular to the molecular axis, is very similar to results

(27) (a) Holladay, A.; Leung, P.; Coppens, P. *Acta Crystallogr.* **1983**, *A39*, 377–387. (b) Clemente, D.; Biagini, M. C.; Rees, B.; Hermmann, W. *Inorg. Chem.* **1982**, *21*, 3741–3749. (c) Martin, M.; Rees, B.; Mitschler, A. *Acta Crystallogr.* **1982**, *B38*, 6–15. (d) Leung, P.; Coppens, P. *Acta Crystallogr.* **1983**, *B39*, 535–542.

(28) Chatt, J.; Duncanson, L. A.; Venanzi, L. M. *J. Chem. Soc.* **1958**, *3*, 3203–3207.

(29) (a) Goddard, R.; Krüger, C. *Electron Distributions and the Chemical Bond*; Coppens, P., Hall, M. B., Eds.; Plenum Press: New York, 1982; pp 297–330. (b) Krüger, C.; Goddard, R.; Claus, K. H. *Z. Naturforsch.* **1983**, *38b*, 1431–1440.

(30) Spasojević-de Biré, A.; Nguyen Quy Dao; Strich, A.; Thieffry, C.; Bénard, M. *Inorg. Chem.* **1990**, *29*, 4908–4915. (b) Low, A.; Hall, M. B. *Organometallics* **1990**, *9*, 701–708.

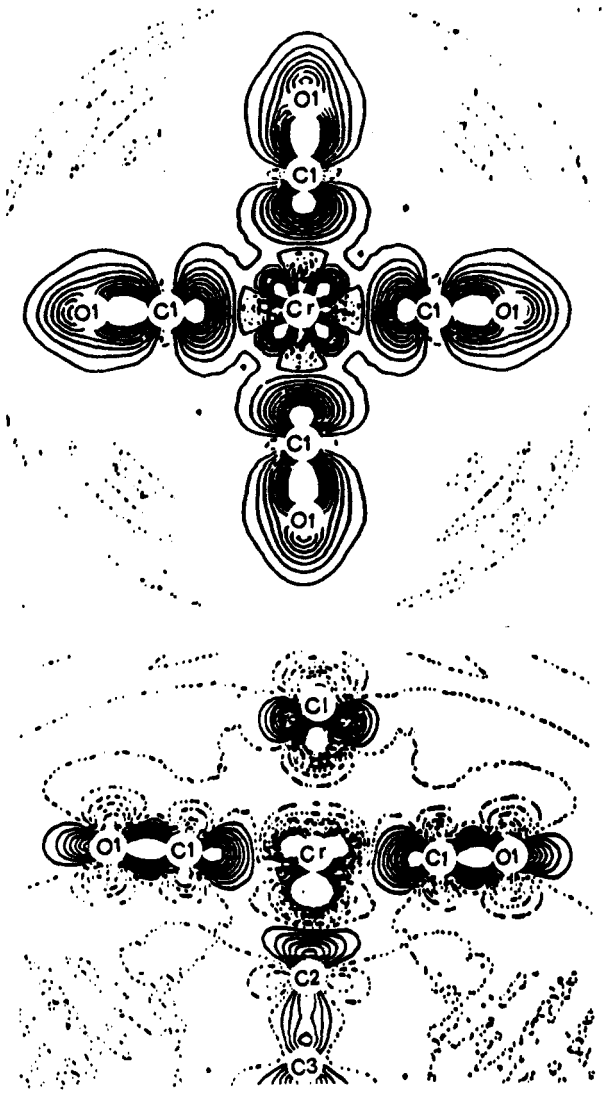

Figure 6. Static deformation density with contours 0.1 e·Å^{-3}: (a, top) Plane containing the four carbonyl groups; (b, bottom) plane containing the carbynic bond and two carbonyl groups.

Figure 7. Conjugation effect demonstrated by static deformation density with contours 0.1 e·Å^{-3}: (a, top) Plane containing the carbynic bond and the phenyl ring; (b, bottom) plane containing the carbynic bond and perpendicular to the phenyl plane.

Table IV. Chromium Parameters[a]

multipole populations		d orbital populations			
	C_{4v}		C_{4v}		C_{2v}
P_{10}	−0.09(3)	dz^2	0.39(4)	8%	0.41(5)
P_{20}	−0.63(2)	d_{xz}			0.65(5)
P_{30}	0.44(4)	d_{yz}			0.58(4)
P_{40}	0.04(2)	$d_{xz} + d_{yz}$	1.23(3)	25%	
P_{44+}	−0.36(2)	$d_{x^2-y^2}$	1.09(3)	22%	1.10(9)
		d_{xy}	2.23(3)	45%	2.22(7)
		$d_{z^2}/d_{x^2-y^2}$			0.3(1)
		total	4.92(7)		5.3(2)

[a] The local symmetry used for the refinement is precised.

obtained for covalently bound fluorine and chlorine atoms.[31] It may reflect a preferential occupation of the p_x and p_y orbitals (i.e. in the directions perpendicular to the Cr–Cl bond). This density actually has the shape of a ring around the chlorine ion. It should be noted that the theoretical calculations[30] show very weak deformations in this region and in rather good agreement with the experimental study of the methylated chromium carbyne complex II. There was already evidence of the *trans* effect (the four carbonyl groups are bent toward the chlorine atom), so the fact that the deformation density of the chlorine atom has this shape is a direct proof of the *trans* effect between the chlorine and the C(carbyne) atoms.

Concerning the Cr–C(carbyne) bond, the shape of the electron deformation density tends to show that the Cr–C(carbyne) bond is characterized by a very diffuse electron deformation density. An exess of density in the C–C bond of the carbynic ligand appears only in the X–M map but still as quite a weak signature. One reason can be evoked for this feature: As we have already mentioned, the Cr–C(carbyne) is located on the symmetry axis; therefore the experimental error is higher[25] thus affecting the electron deformation density. On the contrary, in the dynamic multipole map (Figure 5b) and especially in the static multipole map (Figure 6b), the Cr–C(carbyne) bond is much clearer. The differences between these last two maps are mainly due to the deconvolution of the atomic thermal motions leading to a definite sharpening of the peaks. The discussion below will be based on the static deformation-density maps. The Cr–C(carbyne) bond has a gourd form, the larger part of which is oriented toward the carbon atom. This bond does not have a revolution symmetry around its binary symmetry axis. This is attributed to the conjugation effect, which will be discussed in the next section. The C(carbyne)–C(phenyl) bond is classical and does not show any particular feature in the deformation density.

Concerning the phenyl group, the rigid fragments analysis for neutron results has already shown that it undergoes large amplitude librations.[7] This phenomenon is observed thanks to the very peculiar electron density in this part of molecule: in the deformation-density maps, the density is averaged over the positions of the atoms during the rocking movements of this

(31) (a) Oelkrug, D. *Structure and Bonding*; Hemmerich, P., Jørgenson, C. K., Neilands, J. B., Nylholm, R. S., Reinen, D., Williams, R. J. P., Eds.; Springer-Verlag: Berlin, 1971; Vol. 9, pp 1–26.

Table V. Qualitative and Quantitative Comparison of Bonds for I and II[a]

	shape		eccentricity		peak height (e·Å^{-3})		interatomic dist (Å)	
	I	II	I	II	I	II	I	II
Cr—Cl	2 peaks ⊥ to the bond axis	peak on the bond axis			1.0	0.3	2.409(1)	2.442(1)
Cr—C	ellipse	ellipse	1.9–1.1	1.6–1.5	0.5	>1.0	1.957(1)	1.978(3)
								1.928(3)
C≡O	ellipse	ellipse	1.6–0.9	1.5–1.3	>1.0	>1.0	1.133(1)	1.147(4)
								1.128(4)
free oxygen doublet	ellipse		0.7		0.8			
Cr≡C	ellipse	ellipse	2.6–2.0	2.1	0.6	0.8	1.724(1)	1.718(3)
≡C—C	ellipse	ellipse	0.5–0.8	1.4	0.4	1.0	1.423(1)	1.456(5)

[a] Eccentricity: ratio of major axis of the ellipse (perpendicular to the bond axis) to the minor axis of ellipse (along the bond axis). All these data are collected from the static deformation map.

fragment about the rotational center. Since our model is limited to linear, harmonic vibrations, we cannot expect to deconvolute the effect of thermal motions correctly. The charge density of this group will therefore not be discussed.

2.3. Net Charge and Multipole Populations. We shall now consider the multipole model parameters. The κ-values, atomic net charges (Table III), and, in the case of the chromium atom, the multipole populations (Table IV) are reported. The chromium appears as close to a +1 ion, the chlorine is almost neutral, the carbonyl groups are slightly negative (≈–0.5 electrons), and the phenylcarbyne has a net charge of +0.1. Although the unit cell is constrained to be neutral the algorithm used gives an estimate of the effect of releasing this constraint: the number of valence electrons would only decrease from 86 to 85.5 per molecule.

For chromium (Table IV) the largest population coefficient is P_{30}. This may be explained by a $4p_z$–$3d_{z^2}$ hybridization stabilized by the formation of the Cr–C–Ph triple bond. This means that an interpretation of the multipole parameters in terms of d-orbital populations within a crystal field approximation is not rigorously justified. We nevertheless report the result of such an exercise (Table IV) which further shows the nonvalidity for the present compound: the d_{xy} level is overpopulated (2.2 electrons). This is different from the analysis of the corresponding Cr–C methyl compound where the Y_{30} multipole has a low population, and the resulting d-orbital occupations come out in quite close agreement with theory.

2.4. Conjugation Effect in the Cr≡C–Phenyl System. The discussion is based on the static deformation-density maps (Figure 7), but the same conclusions can be drawn from the X–M maps. The peak in the C–C "single" bond is broader in the plane perpendicular to the phenyl ring, whereas the chromium–carbon "triple" bond has its largest extent in the plane parallel to the phenyl ring. This is a consequence of a conjugation effect between the phenyl ring and the triple bond. This has previously been demonstrated by analyzing the force field by vibrational spectroscopy.[32] From the force constants one can evaluate the bond order in this molecule. It is less than three (≈2.7) for Cr≡C and greater than one (≈1.4) for the C–C bond. The deformation observed in I is similar to those observed in organic compounds of the cumulenic family,[33] although for I it preserves the specific shape of an oblate ellipsoid characteristic of the metal–carbyne bond.

Kostic and Fenske[6] have performed the molecular orbital calculations of cationic carbyne complexes. In the case of a CPh^+ fragment, they have suggested that the LUMO (4π) perpendicular to the phenyl ring is stabilized by significant delocalization over the ortho and para positions and, for the orbital 5π, in the plane of the phenyl ring, there is a hyperconjugation effect between the C–C and C–H bonds. These two effects can explain the deformation of the phenyl ring observed in the neutron study.

2.5. Comparative Study of the Chemical Bonds in I and Its Methyl Homolog II. In order to compare qualitatively and quantitatively the bonds common to the complexes I and II we have compiled parameters describing the bond densities in Table V. In the two complexes, the experimental density maps present a strong similarity of the carbynic bond shape. It is therefore particularly interesting that two ab-initio calculations[30a,b] for complex II have led to a carbynic bond with a shape which is strikingly similar to that of the experimental results.

Both the observed and calculated density patterns for the metal–carbon triple bond are similar to the one obtained for the metal–carbonyl bonds. These two metal–ligand interactions may be considered of the same type. The coordination of carbon monoxide is classically described in terms of a ligand σ-donation and a metal π-back-donation. Orbital interaction diagrams[29a] suggest that the bonding of the carbyne to the metal fragment is not different in this respect, only the strength of the π-back-donation interaction is much stronger leading to a near-equal sharing of the electrons between overlapping atomic orbitals.[34] We may quantify this observation by calculating the eccentricity of the ellipsoid shape peaks (Table V). The eccentricity is greater than two for the Cr≡C bond and less than two for the Cr–C(CO) bond corroborating the idea that the back-donation toward the carbyne carbon is stronger than toward the carbonyl ligands. Furthermore, the average of the two eccentricities of I in the two perpendicular planes (≈2.3) is greater than that observed for II (≈2.1) indicating that the back-donation, as expected, is stronger for the phenyl complex than for the methyl complex.

Because of the limited resolution of the diffraction study ($(\sin\theta)/\lambda \leq 0.7$ Å^{-1}), the free oxygen lone pair are not present on the map for II. It is however possible to detect a density of 0.1 e.Å^{-3} when refining the κ' expansion–contraction coefficient (eq 1). For compound I, the free oxygen doublets appear clearly on the static map but are weaker and more diffuse on the X–M map, due to the strong thermal movement of this part of the molecule.

In complex II the carbonyl group (C1O1) is tilted in the direction of the chlorine atom (angle Cl–Cr–O1 = 86.6°) whereas the two groups (C2O2 and C4O4) are practically coplanar (angle Cl–Cr–O2 = 89.6° and angle Cl–Cr–O4 = 90.2°) and the last (C3O3) is turned in the direction of the methyl group (angle Cl–Cr–O3 = 91.2°). In the phenylcarbynic complex, all of the carbonyl groups are turned toward the halogen atom (angle Cl–Cr–O1 = 86.9°). The theoretical work of Kostic and Fenske[6] has shown that the carbonyl ligands orient toward the weakest π-acceptor or the strongest donor group. One would imagine that the chlorine atom is a better donor group than the organic radical except if the latter is in a more favorable position: this

(32) (a) Février, H. Thesis, University of Paris XIII, France, 1982. (b) Nguyen Quy Dao; Fischer, E. O.; Kappenstein, C. *Nouv. J. Chim.* **1980**, *4*, 85–94. (c) Nguyen Quy Dao; Fischer, E. O.; Lindner, T. L. *J. Organomet. Chem.* **1981**, *37*, 1087–1092. (d) Nguyen Que Dao; Fevrier, H.; Jouan, M.; Fischer, E. O.; Röll, W. *J. Organomet. Chem.* **1984**, *275*, 191–207.
(33) Irngartinger, H. *Electron Distribution and the Chemical Bond*; Coppens, P., Hall, M. B., Eds.; Plenum Press: New York, 1982; pp 361–379.
(34) Poblet, J. M.; Strich, A.; Wiest, R.; Bénard, M. *Chem. Phys. Lett.* **1986**, *126*, 169–175.
(35) Jonhson, C. K. ORTEP II; Report ORNL-5138; Oak Ridge National Laboratory, Oak Ridge, TN, 1976.

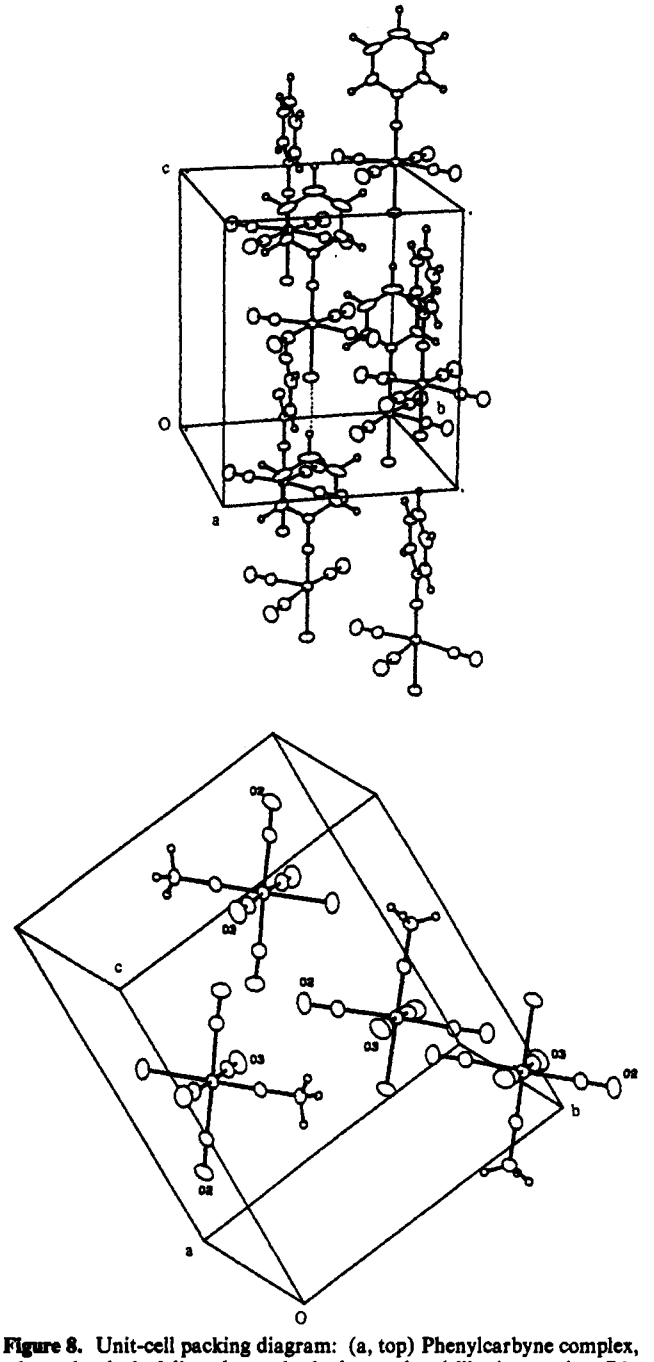

Figure 8. Unit-cell packing diagram: (a, top) Phenylcarbyne complex, where the dashed line shows the hydrogen bond-like interaction C6–H6···Cl–Cr; (b, bottom) methylcarbyne complex.

is the case with the bond (C6–H3) and the carbonyl group (C3–O3) in an eclipsed position. However the different orientations observed for the carbonyl groups may also be due to crystal packing effects (Figure 8). Nevertheless it seems reasonable for the orientation of the carbonyl groups to have an influence on the C–Cl bond. As a matter of fact, one observes a longer interatomic distance for the methylcarbynic complex, where there is only one group which interacts with the halogen atom, than when there are four ligands (complex I). The influence of the hydrogen bond-like interaction C6–H6···Cl–Cr of the phenylcarbynic complex[7] on the bond length is certainly weaker, and the dominating factor must be the interaction with the carbonyl groups.

One of the important results we have established is that we have found experimental differences in the chemical bonds in two similar complexes I and II: the phenyl group induces a stronger back-donation effect between the carbynic carbon and the metal, and the stabilization of the C–C bond has increased with the conjugation effect. In order to point out the interest of such results for the organometallic field, we quote a catalytic study which has demonstrated differences in reaction between I and II. Katz *et al.*[4] studied the polymerizations of acetylenes and cyclic olefins induced by metal carbynes. They observed that the phenylcarbyne initiator (M = W, X = Br, [acetylene]/[initiator] = 5367, time = 92 h, 34% yield, T = 297 K) was a better catalyst compared to the methylcarbyne compound (the phenyl group is replaced by a methyl group, M = W, X = Br, [acetylene]/[initiator] = 333, time = 11 days, 11% yield, T = 258 K).

Conclusion

This is one of the first experimental studies on the electron density of a organometallic compound crystallizing in a non-centrosymmetric system which has been determined by a multipolar atom model using both X-ray and neutron diffraction results. The electron density is particularly demonstrative, concerning the back-donation, the new metal–carbyne bond, the *trans* effect, and the conjugation effect. These features confirm the results already obtained with a centrosymmetric compound, whose electron density structure was also determined accurately with the same multipolar models, and especially the specific features obtained previously by ab-initio calculations. This work shows that the deformation density can be applied advantageously in the study of organometallic compounds in order to understand the nature of the chemical bonds.

Acknowledgment. The authors thank M. Bonnet (SPRSM) and H. Février and D. Neugebauer (Laboratoire PCM) for collecting the data and C. Lecomte (Laboratoire de Minéralogie, Cristallographie et Physique Infrarouge), who invited one of us (A.S.-d.B) for a study in this Laboratory. They also thank P. J. Becker (Laboratoire de Minéralogie et Cristographie, Paris) and F. Baert (Laboratoire de Physique Fondamentale, Lille, France) for constructive discussions. The calculations have been done on the IBM-4381 of the Centre de Traitement de l'Information de l'Ecole Centrale Paris; we thank the staff for their cooperation.

Supplementary Material Available: Tables of atomic positions (Table S1, thermal parameters (Table S2), and multipole populations (Table S3) of the three X-ray refinements and a figure showing the local Cartesian axis systems defined for each atom of the multipole model (Figure S4) (12 pages). Ordering information is given on any current masthead page.